


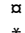
## RESEARCH ARTICLE

## Segregational drift hinders the evolution of antibiotic resistance on polyploid replicons

Ana Garoña<sup>1</sup><sup>✉</sup>, Mario Santer<sup>1,2</sup><sup>✉</sup>, Nils F. Hülter<sup>1</sup>, Hildegard Uecker<sup>2\*</sup>, Tal Dagan<sup>1\*</sup>

**1** Institute of General Microbiology, Kiel University, Kiel, Germany, **2** Research group Stochastic Evolutionary Dynamics, Department of Evolutionary Theory, Max Planck Institute for Evolutionary Biology, Plön, Germany

 These authors contributed equally to this work.

 Current address: Instituto Gulbenkian de Ciência, Oeiras, Portugal

\* uecker@evolbio.mpg.de (HU); tdagan@ifam.uni-kiel.de (TD)



## Abstract

The emergence of antibiotic resistance under treatment depends on the availability of resistance alleles and their establishment in the population. Novel resistance alleles are encoded either in chromosomal or extrachromosomal genetic elements; both types may be present in multiple copies within the cell. However, the effect of polyploidy on the emergence of antibiotic resistance remains understudied. Here we show that the establishment of resistance alleles in microbial populations depends on the ploidy level. Evolving bacterial populations under selection for antibiotic resistance, we demonstrate that resistance alleles in polyploid elements are lost frequently in comparison to alleles in monoploid elements due to segregational drift. Integrating the experiments with a mathematical model, we find a remarkable agreement between the theoretical and empirical results, confirming our understanding of the allele segregation process. Using the mathematical model, we further show that the effect of polyploidy on the establishment probability of beneficial alleles is strongest for low replicon copy numbers and plateaus for high replicon copy numbers. Our results suggest that the distribution of fitness effects for mutations that are eventually fixed in a population depends on the replicon ploidy level. Our study indicates that the emergence of antibiotic resistance in bacterial pathogens depends on the pathogen ploidy level.

 OPEN ACCESS

**Citation:** Garoña A, Santer M, Hülter NF, Uecker H, Dagan T (2023) Segregational drift hinders the evolution of antibiotic resistance on polyploid replicons. *PLoS Genet* 19(8): e1010829. <https://doi.org/10.1371/journal.pgen.1010829>

**Editor:** Ivan Matic, Institut Cochin, FRANCE

**Received:** February 2, 2023

**Accepted:** June 14, 2023

**Published:** August 3, 2023

**Copyright:** © 2023 Garoña et al. This is an open access article distributed under the terms of the [Creative Commons Attribution License](https://creativecommons.org/licenses/by/4.0/), which permits unrestricted use, distribution, and reproduction in any medium, provided the original author and source are credited.

**Data Availability Statement:** The source data underlying Figs 1 and 2 and Figs S1, S2, S3, S4, S5 and S6 are provided as a Source Data file. The code for our simulations is available online (<https://github.com/mariosanter/multicopy-bottle-fixation>).

**Funding:** AG is supported by the International Max Planck Research School (IMPRS) for Evolutionary Biology. TD is supported by the Leibniz Science Campus EvoLUNG. MS is a member of the International Max Planck Research School for Evolutionary Biology and gratefully acknowledges the benefits provided by the program. This work was furthermore funded by the Deutsche

## Author summary

Prokaryotic replicons—chromosomes and plasmids—may be present in the cell in multiple copies, a phenomenon termed polyploidy. Here we studied the effect of replicon copy number, i.e., polyploidy level, on the emergence of beneficial traits in prokaryotes, with a focus on the evolution of antibiotic resistance. We discovered that beneficial mutations encoded in multicopy replicons are bound to be frequently lost due to stochasticity during cell division that ultimately increases genetic drift. Our study presents empirical evidence for the effect of polyploidy on the rate of adaptation in prokaryotes. A comparison to simulations of a mathematical model confirms our understanding of the allele dynamics. We

Forschungsgemeinschaft (DFG, German Research Foundation) - project number 418432175 (to HU) and European Union (ERC) pMolEvol, grant number 101043835 (to TD). The funders had no role in study design, data collection and analysis, decision to publish, or preparation of the manuscript.

**Competing interests:** The authors have declared that no competing interests exist.

conclude that drug treatment strategies against pathogenic bacteria should consider the ploidy level of the organism.

## Introduction

Bacterial adaptation to novel environmental conditions depends on the availability of beneficial alleles and the dynamics of their proliferation within the population. However, novel alleles are initially rare in the population and therefore—even if they are adaptive—prone to stochastic loss due to genetic drift [1]. The probability that beneficial alleles survive the early proliferation phase and become established is termed 'establishment probability'. The probability of establishment (and eventually fixation) of beneficial alleles is a key concept in theoretical population genetics [2,3], dating back to the very early days of the field [1]. Understanding the determinants of allele establishment in bacterial populations is pivotal in the context of antibiotic resistance evolution. Antibiotic treatment confers a growth advantage to bacteria carrying resistance alleles, which might establish and subsequently rise to high numbers. The emergence of novel resistant strains of diverse human and livestock pathogens due to antibiotic treatment has worrisome consequences for global human health [4]. Sustainable treatment strategies are needed [5], for the development of which a profound understanding of the dynamics of beneficial alleles—including the early stochastic phase—is necessary. Several recent studies have supplied empirical evidence for stochastic loss of adaptive antibiotic resistance genotypes and factors that may be involved in their establishment [6–8]. However, the effect of bacterial ploidy on the establishment of antibiotic resistance remains understudied.

Prokaryotic genomes comprise chromosomes and extrachromosomal genetic elements, e.g., plasmids, collectively termed replicons. The number of chromosome copies in the cell is tightly controlled during replication and is synchronised with cell division [9,10]. Several prokaryotic taxa are known to harbour polyploid chromosomes. This includes cyanobacteria, e.g., *Synechococcus elongatus* that has a chromosome copy number of 3–4 [10,11]. Other examples are the human pathogens *Borrelia hermsii* and *B. burgdorferi*, which have a chromosome copy number of 4–14 and 10–20, respectively [12]. The number of chromosome copies in the cell may furthermore depend on the growth phase and nutrient conditions (e.g., refs. [13,14]); indeed, also monoploid bacteria, such as *E. coli*, can be polyploid (or rather mero-oligoploid) during exponential growth [15,16]. The number of plasmid copies in a host cell depends on the plasmid type and the host genetics. Low copy number plasmids are found in 1–5 copies in the cell, while high copy number plasmids may reach 200 copies in the cell [17,18]. Similarly to chromosomes, the plasmid copy number may vary depending on the growth conditions [19,20].

The presence of multiple replicon copies in the cell has important implications for bacterial evolution. Experimental evolution of bacteria has shown that the mutational supply is positively associated with the replicon copy number, i.e., the probability of novel mutations can be higher for polyploid replicons (as demonstrated for multicopy plasmids in ref. [21]). Polyploidy furthermore allows for intracellular genetic diversity, also termed heterozygosity [22–24]. Alleles in monoploid chromosomes are inevitably inherited to both daughter cells during cell division. In contrast, the segregation of alleles emerging in one out of many copies of a polyploid replicon is a neutral process and it may be unbalanced, such that only one daughter cell inherits the novel allele. The effect of stochasticity on novel plasmid alleles during cell division has been termed segregational drift [25]. The dynamics of alleles encoded in polyploid chromosomes (and multicopy plasmids) are thus affected by processes at two hierarchical

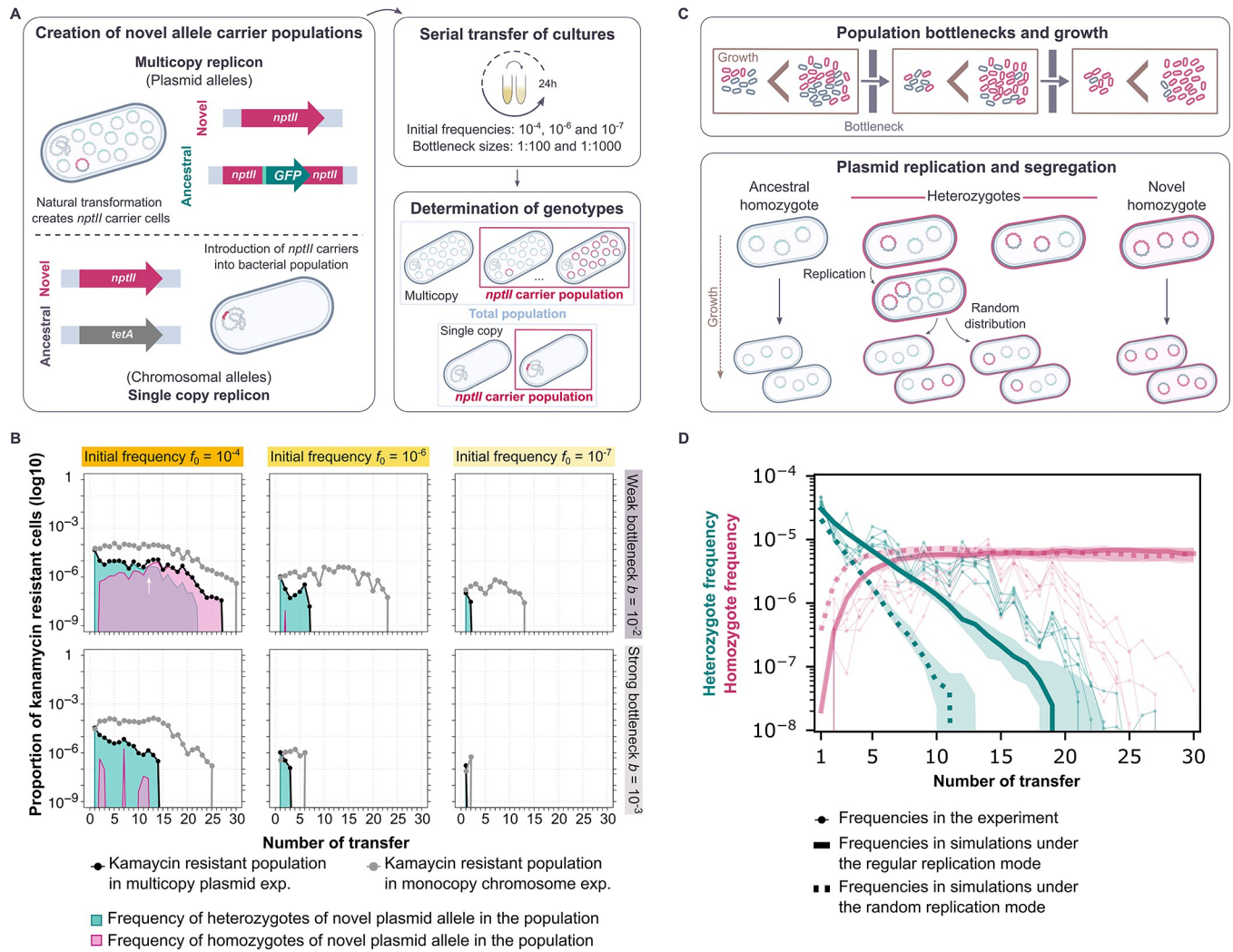
levels: within the cell and within the population [25–29]. The mechanism of replication and the mode of segregation are important determinants of the allele dynamics on polyploid replicons [28,29]. A recent model on the fixation process of beneficial allele dynamics shows that heterozygous cells can persist for an extended period of time during the fixation process of high copy number replicons [29]. The coexistence of multiple plasmid alleles within a cell enables the host population to survive in fluctuating environmental conditions, e.g., under alternating drug pressures selecting for multiple antibiotic resistances [23]. The replicon copy number has furthermore important implications for the dynamics of rare novel alleles. Theory predicts that segregational drift will decrease the establishment probability of beneficial alleles when encoded in multicopy plasmids, at least in the absence of gene dosage effects [25,27]. Nonetheless, empirical evidence for the workings of segregational drift on the dynamics of beneficial alleles remains lacking.

Here we investigate the dynamics of a novel antibiotic resistance allele in an experimentally evolving bacterial population of *Acinetobacter baylyi* and compare the results between populations where the allele is encoded either on a polyploid (multicopy) plasmid or on a monoploid chromosome. In our experimental setup, we manipulate the degree of stochasticity present at the level of the cell population using two measures: 1) introducing a low initial frequency of the novel resistance allele, and 2) applying serial population bottlenecks on the evolved population. This experimental design allows us to systematically study how segregational drift interacts with stochasticity in the population dynamics of cells carrying the novel allele. We furthermore combine the experimental results with a mathematical model of bacterial population genetics that is specifically tailored to the experimental setup to directly probe our mechanistic understanding of the dynamics of alleles on polyploid replicons.

## Results

### Rare alleles in multicopy replicons are prone to rapid loss

To experimentally quantify the effect of the replicon copy number on the fate of beneficial alleles, we studied the dynamics of an allele conferring resistance to the antibiotic kanamycin (*nptII*). The beneficial allele was introduced either on a polyploid (multicopy) plasmid or a monoploid chromosome in the model organism *A. baylyi*. Performing an experimental evolution experiment with serial transfers, we examined the effects of the initial allele frequency (i.e., the number of novel allele copies), the strength of the population bottlenecks, and the selection regime on allele dynamics (Fig 1A). We compare the results for three initial frequencies of cells containing the novel allele:  $f_0 = 10^{-4}$  (ca.  $10^5$  cells, high),  $f_0 = 10^{-6}$  (ca.  $10^3$  cells, moderate), and  $f_0 = 10^{-7}$  (ca.  $10^2$  cells, low). The control of the initial frequency of cells containing the novel plasmid allele was achieved via natural transformation employing varying donor DNA concentrations (700, 7, or 0.7 ng/ $\mu$ l DNA). The novel *nptII* allele is introduced into an ancestral population that carries the stable model plasmid pTAD-R, which has a copy number of ca. 15. Homologous recombination between the donor DNA and the ancestral plasmid creates heterozygous cells carrying both the ancestral and the novel alleles, where the intracellular frequency of the novel allele is one plasmid copy out of 15 due to the one-hit kinetics of natural transformation (Fig 1A; ref. [28]). For the chromosomal allele, we controlled the initial allele frequency by mixing strains carrying either the novel or the ancestral allele at the abovementioned frequencies. Using this approach, we create an ancestral population that has the same initial number of novel allele copies and the same initial frequency of cells carrying the novel allele for the polyploid and the monoploid replicons. The initial novel allele frequency from the total replicons in the population is consequently lower for the plasmid experiments. The evolved populations were serially transferred using two population



**Fig 1. Integrating multicopy replicon allele dynamics *in vivo* and *in silico*.** (A) Our experimental system enables us to create and follow bacterial populations encoding a novel allele in a plasmid or chromosomal replicon over the course of an evolution experiment. The novel allele employed is a kanamycin resistance gene (*npIII*), which encodes aminoglycoside 3'-phosphotransferase II [49]. The ancestral plasmid allele is a green fluorescence protein (*gfp*) whose transcription is under the control of a LacI repressor [28]. The chromosomal ancestral allele is a tetracycline resistance gene (*tetA*). The bacterial populations were serially passaged under different experimental conditions for approximately 200 generations. The frequency of cells carrying the novel allele was followed by selective plating on kanamycin-containing medium, where each viable cell will form a colony. For the plasmid replicon, the presence of both ancestral and novel allele, that is homozygotes and heterozygotes, was distinguished due to fluorescence conferred by the ancestral allele. Bacterial colonies were visually inspected employing blue light. Note that this is an assessment between homozygotic and heterozygotic colonies rather than an exact quantification of the number of alleles present. (B) Allele dynamics of representative populations evolved under non-selective conditions. The white arrow marks the point at which the frequencies of heterozygous and novel homozygous cells are equal. The plots start at the end of the first day of growth, where the final transformant frequencies, according to the amount of donor DNA added, have been achieved. The remaining experimental populations are shown in S3 and S4 Figs. (C) Schematic diagram of the mathematical model of plasmid allele dynamics under periodic population bottlenecks (transfers). Bacterial populations grow until they reach a carrying capacity  $N_c$  before each transfer. A proportion  $b$  of cells is randomly chosen for the next growth phase. During each growth phase, cells carrying only the ancestral allele (ancestral homozygotes) replicate at a rate that is  $1-s$  times smaller than the rate of cells carrying the novel allele (heterozygotes and novel homozygotes). (D) Comparison between the allele dynamics in evolution experiments using the pTAD-R plasmid and in model simulations with replicon copy number  $n_{rc} = 15$  under non-selective conditions ( $s = 0$ ) for high initial frequencies,  $f_0 = 10^{-4}$ , and weak bottlenecks,  $b = 10^{-2}$ . Bold green (red) lines show the median of the heterozygote (homozygote) frequencies before each transfer from 30 simulations for both modes of replication; shaded areas show the corresponding interquartile ranges. Thin lines show the heterozygote frequency from the six replicates of the evolution experiment. Simulation results were obtained by integrating the differential equations for bacterial growth and sampling new populations at each transfer from a multinomial distribution defined by the genotype frequencies at carrying capacity.

<https://doi.org/10.1371/journal.pgen.1010829.g001>

bottleneck sizes: 1:100 ( $b = 10^{-2}$ ; ca.  $10^7$  cells, weak bottleneck) and 1:1000 ( $b = 10^{-3}$ ; ca.  $10^6$  cells, strong bottleneck) for ca. 200 generations for the weak bottleneck and 300 for the strong bottleneck (30 serial transfers). The experiment was conducted with six replicates for each experimental condition. The fitness effect of the novel plasmid allele in the absence of antibiotics was estimated from the relative fitness of cells that are homozygous for the novel allele and cells that are homozygous for the ancestral allele; the results show a mean relative fitness of  $w = 0.9884 \pm 0.0224$  SD (or selective coefficient of  $s = -0.0116$ ), which was not significantly different from  $w = 1$  (or  $s = 0$ ;  $p = 0.4375$ , using Wilcoxon test,  $n = 6$ ; S2 Fig). The novel chromosomal allele had a mean relative fitness of  $w = 0.9892 \pm 0.0086$  SD, with no significant difference from  $w = 1$  (i.e.,  $s = 0$ ;  $p = 0.0625$ , using Wilcoxon test,  $n = 6$ ; S2 Fig). Thus, in the absence of antibiotics, changes in allele frequencies in the population over time are expected to stem from neutral processes rather than fitness differences between genotypes in the population. Changes in the allele frequency due to horizontal transfer via natural transformation are negligible in our system [28].

To demonstrate the effects of the initial frequency of cells carrying the novel allele and the bottleneck strength, we first present the observed allele dynamics under non-selective conditions for a set of representative populations (Fig 1B). Note that the novel allele has no significant fitness effect under neutral conditions (S2 Fig). Our results show that with a high initial frequency ( $f_0 = 10^{-4}$ ) and a weak bottleneck ( $b = 10^{-2}$ ), the dynamics of the novel allele in both plasmid and chromosome are characterized by a stable persistence during the first ca. 20 transfers, followed by a decrease in the fraction of kanamycin-resistant cells (i.e., mutant cells). An eventual decrease in the frequency of the rare novel allele in the population is to be expected under genetic drift; the fixation probability of a neutral allele corresponds to the initial allele frequency and is thus very low [30]. Segregation of polyploid replicon copies reduces the number of mutant cells (through flux into the two homozygous cell types) and thus increases the effect of stochasticity. Indeed, the frequency of kanamycin-resistant cells decreases faster if the allele is on the multicopy plasmid than if it is on the chromosome (Fig 1B). At the end of the experiment, the novel plasmid allele was lost in most replicates, while the chromosomal allele was present in the population at a frequency of ca.  $5 \times 10^{-7}$ .

Our system enables us to distinguish between heterozygous and homozygous cells for the novel plasmid allele. The subpopulation of cells that carries the novel allele initially consists of heterozygotes in which the novel allele is present in only one plasmid copy per cell. Over the course of the experiment, heterozygotes decay due to the random distribution of plasmid copies at cell divisions, which eventually causes the loss of heterozygous cells. For the highest initial frequency,  $f_0 = 10^{-4}$ , kanamycin-resistant homozygous cells arise due to segregational drift and are maintained over several transfers if the applied bottlenecks are weak ( $b = 10^{-2}$ ). Our results show that when the initial frequency of the cells carrying the novel allele is lower, the novel allele is maintained in the population for shorter times (Fig 1B;  $f_0 = 10^{-6}$  and  $f_0 = 10^{-7}$ ).

The bottleneck size applied during the experiment has a significant effect on the allele dynamics, which are characterized by a rapid loss in the populations transferred with a strong bottleneck ( $b = 10^{-3}$ ) compared to those populations evolved with a weak bottleneck. Note that with a strong bottleneck, fewer cells are transferred than with a weak bottleneck, increasing the strength of drift. At the same time, the bottleneck applied also has an effect on the number of generations elapsed, as with the stronger bottleneck more cell divisions will occur until the carrying capacity is reached. Therefore, the loss of the novel allele is more rapid (in terms of number of transfers) when a strong bottleneck is applied. To sum up, under non-selective conditions, both plasmid and chromosomal alleles decrease over time and eventually are lost in most populations by the end of the experiment. Nonetheless, the loss of the plasmid allele is faster in all tested combinations of initial frequencies and population bottlenecks. Our results

are in agreement with previous observations on the effect of segregational drift on the dynamics of alleles encoded in polyploid replicons [25,27,28].

### Mathematical modelling generates predictions on the plasmid replication mode based on the empirical plasmid allele dynamics

To formulate the theoretical expectation for the allele dynamics in the experiments, we adapted a previous mathematical model of vertical replicon inheritance in bacterial populations to match the experimental design of the evolution experiment (Fig 1C; refs. [27,29]). The genotype of a cell is defined by the number of novel and ancestral replicon copies at cell birth, with the total number of novel replicon copies ranging between 0 and the replicon copy number  $n_{rc}$ . Cells in the simulations of monoploid replicons ( $n_{rc} = 1$ ), such as the chromosome in *A. baylyi*, harbor either the ancestral or the novel allele. Cells in the simulations of multicopy replicons ( $n_{rc} > 1$ ), e.g., model plasmid pTAD-R, can be homozygous for the ancestral or for the novel allele, or heterozygous, carrying both allele variants in various proportions. We consider thus all  $n_{rc}+1$  possible cell types. Our model includes two possibilities for the mode of replication: under the *regular replication* mode, all  $n_{rc}$  replicon copies are duplicated before a cell divides. Under the *random replication* mode, single copies are selected randomly for replication in a repetitive process until the cell carries  $2 \times n_{rc}$  copies (refs. [27,29]; see Methods for details). For either mode of replication, the replicon copies are distributed randomly into the two daughter cells at cell division (similarly to pTAD-R), where each cell inherits  $n_{rc}$  copies. Population growth between bottlenecks is modelled by deterministic logistic growth, where we only account for cell replication but not for cell death. At bottlenecks, cells are randomly sampled, introducing stochasticity (see detailed model description in the methods).

The replication mode of the pTAD-R backbone has not been examined experimentally so far. To determine which modelled mode of replication better matches the experimental system, we simulated the segregation dynamics of a novel allele carried by a polyploid replicon and compared the simulated dynamics to the experimental results. The simulation was performed for both replication modes under neutrality ( $s = 0$ ) with a replicon having  $n_{rc} = 15$ , as model plasmid pTAD-R. In this simulation, we opted for the highest initial frequency,  $f_0 = 10^{-4}$ , and the weak bottleneck,  $b = 10^{-2}$ , where stochastic effects other than segregational drift are weakest. The model results show that the frequency of heterozygous cells rapidly decreases at a constant rate, while the frequency of homozygotes first increases and then reaches an equilibrium around transfer 15 (Fig 1D). The comparison between the frequency of heterozygotes and homozygotes from simulations under the mode of regular replication and the experimental results shows a good qualitative agreement for the first 11 transfers (Fig 1D). From transfer 12 onwards, the model underestimates the frequency of heterozygous cells by up to ten-fold. The deviation between the model prediction of the homozygotes frequency and the experimental results increases from transfer 15 when the homozygotes frequency in the experiment decayed. Simulations using the random replication mode overestimate the decay of heterozygotes' frequency as well as the increase in homozygotes' frequency already during the very first transfers (Fig 1D). To test for possible reasons for the observed deviations, we performed further simulations under the regular replication mode, assuming a different plasmid copy number ( $n_{rc}$  between 10 and 30) or a slight negative fitness effect of 1–5% of the novel allele. Increasing the copy number in the simulations yields a better fit to the heterozygote frequencies (S1A Fig); nonetheless, the experimental quantification of pTAD-R copy number does not suggest a large deviation from  $n_{rc} = 15$  [28]. Simulations with a negative selection parameter (approximately between  $s = -0.01$  and  $s = -0.03$ ) yield a better fit to the homozygote frequency observed in the experiment (S1B Fig). Indeed, while the experimental results suggested no significant fitness

effect of the novel plasmid allele, the average relative fitness suggested a slight deviation from a neutral regime (S2 Fig). Note that random replication always entails faster segregation dynamics than regular replication [29]. Hence achieving a good fit between the simulation with random replication and the experimental results would require a substantial increase in the plasmid copy number beyond the experimental evidence for pTAD-R. Consequently, we opted to use the regular replication mode for further simulations of pTAD-R allele dynamics. The correspondence between the simulation results under the regular replication mode and the allele dynamics in the evolution experiment suggests that the replication of plasmid pTAD-R is not random and may follow a regular mode of replication.

### Beneficial alleles on polyploid replicons are prone to loss due to segregational drift

To examine the effect of replicon polyploidy on the dynamics of beneficial alleles, we experimentally evolved the bacterial populations under conditions where the novel allele is beneficial, i.e., under selection for kanamycin resistance. In order to identify a comparable selection regime for both replicon types, we quantified the fitness effect of the *nptII* allele when encoded in the multicopy plasmid or single copy chromosome, employing increasing kanamycin concentrations (S5 and S6 Figs). During the evolution experiment, we applied a constant antibiotic pressure, which confers cells that are homozygous for the novel allele a fitness benefit of ca. 10% (i.e., selection coefficient  $s = 0.1185 \pm 0.0415$  SD for the novel resistant strain). The concentration of antibiotics employed to achieve a fitness benefit of ca. 10% in multicopy and single-copy replicon in novel homozygotes is similar. Therefore, we assume that the effect of gene dosage in our system is negligible; that is having more than one copy (1 to 15 copies) does not produce a higher fitness benefit to the bacteria at the concentrations employed. Note that the effect of selection is restricted to processes at the population level; antibiotic selection has no known effect on plasmid replication and segregation. We examined the effect of selection on the dynamics of the novel allele in combination with the effect of initial frequency and population bottleneck size. For each replicon type, we thus tested a total of 12 parameter combinations, each with 6 replicates (Figs 2, S3 and S4).

We first focus on the results for the plasmid-encoded allele. As expected, the novel allele is maintained for longer and lost less often under selection than under neutral conditions. With high initial frequencies ( $f_0 = 10^{-4}$ ), the fraction of kanamycin-resistant cells increased in the population over time, regardless of the population bottleneck (Fig 2A, plots 1,3). The frequency of cells that carry the novel allele at the end of the experiment is close to the fixation threshold (that was set to 90%) in most replicates. In contrast, at low or moderate initial frequencies, the novel plasmid allele was quickly lost in most populations (Fig 2A). In populations that evolved under weak bottlenecks, the novel plasmid allele is lost in 1 out of 6 replicates for moderate initial frequencies and in 4 out of 6 replicates for low initial frequencies (Fig 2A, plots 5,9). In some replicate populations where the allele is maintained, we observed a slow decrease in the fraction of kanamycin-resistant cells from the 20<sup>th</sup> transfer on. Under the strong bottleneck, none of the replicate populations maintained the novel allele for moderate or low initial frequencies (Fig 2A, plots 7,11).

The combination of selection and initial frequency has an effect also on the proportion of homozygous and heterozygous cells within the resistant sub-population. For high initial frequency ( $f_0 = 10^{-4}$ ) under selective conditions, the frequency of cells that are homozygous for the novel allele increases rapidly and reaches a similar frequency to that of the heterozygotes within ca. 5–10 transfers (Fig 2B, plots 2.2 and 2.6). This initial rise in frequency is faster in comparison to that observed under non-selective conditions (ca. 10–15 transfers; Fig 1B).





To further examine the effect of polyploidy on the dynamics of novel alleles, we compared the dynamics observed for the plasmid-encoded allele to those observed for the chromosome-encoded allele. When the allele is encoded on the plasmid, the fraction of kanamycin-resistant cells increases more slowly and the time to fixation is longer in comparison to the chromosome-encoded allele (Fig 2C). The slower increase of the frequency of kanamycin-resistant cells in the experiments with the plasmid-encoded allele is best observed at mid-experiment (ca. transfer 15) for the high initial frequency ( $f_0 = 10^{-4}$ ), where the frequency of kanamycin-resistant cells is 100 times lower in comparison to the chromosome experiment. At the end of the experiment, the kanamycin resistance phenotype was fixed in a single population within the plasmid experiment, in contrast to the chromosome experiment where the resistance phenotype was fixed in the majority of populations (Fig 2A and 2C, plots 1,3). At lower initial frequencies ( $f_0 = 10^{-6}$ ,  $f_0 = 10^{-7}$ ), the differences between the frequency of kanamycin-resistant cells observed in the plasmid and chromosome experiments are even more pronounced, with up to ca. 1000-fold in favour of the chromosome populations (Fig 2A and 2C, plot 5). The most striking difference between plasmid and chromosome experiments is observed in populations that evolved under a strong bottleneck ( $b = 10^{-3}$ ). In those populations, the plasmid-encoded allele is lost in all replicate populations (Fig 2A and 2C, plots 7,11), in contrast to the chromosome experiment where the allele is maintained. To conclude, the opposing effects of segregational drift and selection lead to longer fixation time and loss of plasmid alleles in comparison to chromosomal alleles. Our results demonstrate that segregational drift has a pivotal role in the evolution of polyploid replicons.

An alternative explanation for the observed loss of the novel beneficial plasmid allele could be the adaptation of the originally kanamycin-sensitive cells to the antibiotic environment, such that the novel allele is no longer beneficial. To rule out this alternative, we performed a competition experiment where the ancestral kanamycin-resistant populations competed against the evolved kanamycin-sensitive populations (S7 Fig). Our results show that the evolved kanamycin-sensitive populations still had a lower fitness under selective conditions compared to the ancestral kanamycin-resistant populations. Consequently, we conclude that the dynamics of the novel plasmid allele observed during the evolution experiment are the result of plasmid allele segregation rather than adaptation of the kanamycin-sensitive population to kanamycin.

### The negative effect of segregational drift on the fixation of the beneficial allele is predicted by model simulations

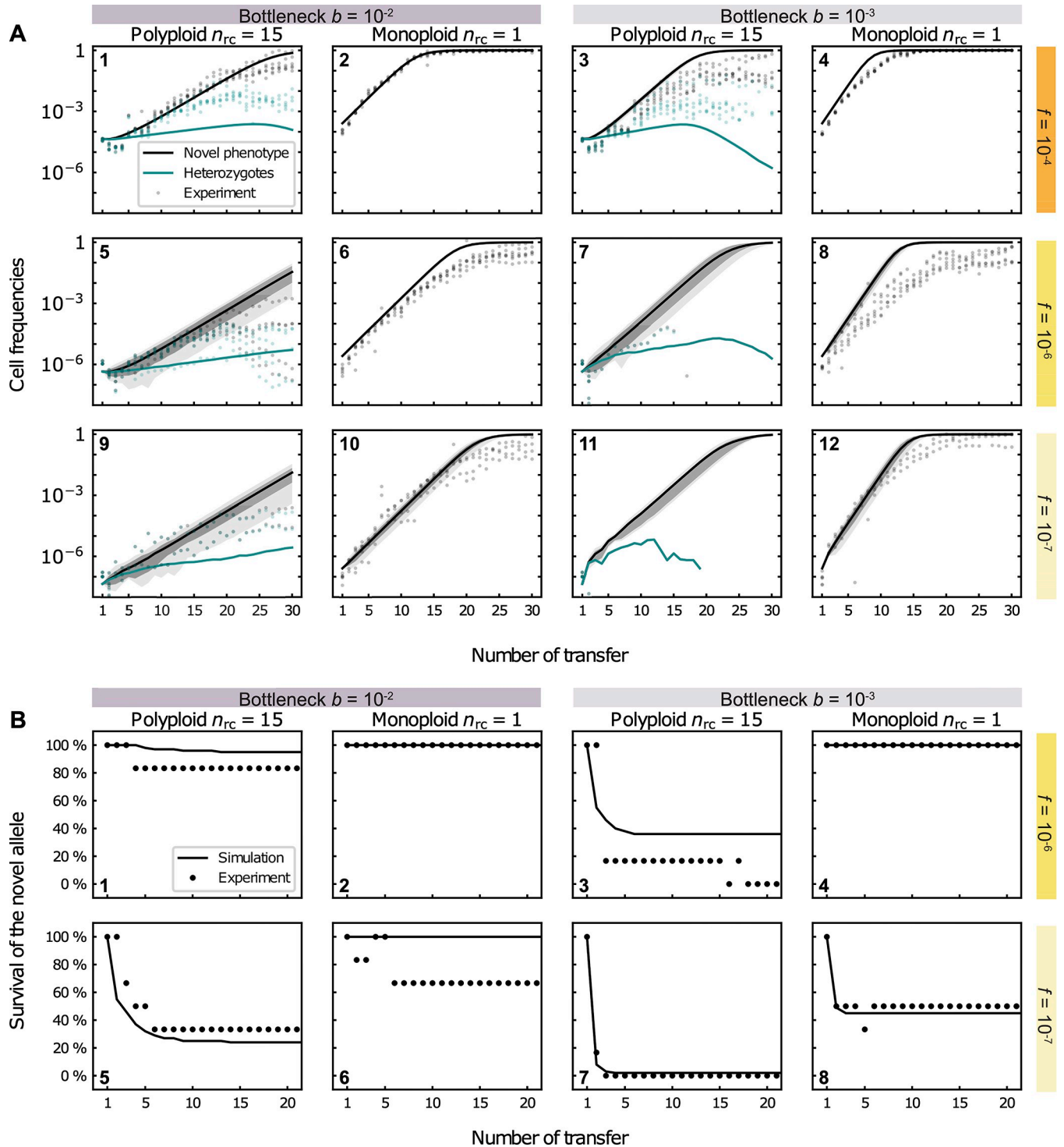
The experimental results in the previous sections are in line with previous theoretical predictions on the effects of replicon polyploidy on the dynamics of beneficial alleles [27]. For a direct comparison of the experimental results to theoretical predictions, we performed simulations with the model that is adapted to the experimental set-up. In our simulations, we assume that cells carrying only the ancestral allele replicate at a rate  $1-s$ , and cells carrying at least one copy of the novel allele replicate at a rate 1. The model assumes no effect of gene dosage.

To obtain a selection parameter that optimally reflects the allele dynamics over the entire duration of the experiment, we first estimated the parameter  $s$  from the mean frequencies of the kanamycin-resistant subpopulation in the evolution experiment for large initial frequencies ( $f_0 = 10^{-4}$ ) and weak bottlenecks ( $b = 10^{-2}$ ). The  $s$  parameters yielding an optimal fit between the simulated dynamics of the novel allele and the corresponding dynamics were selected for further simulations (S8 Fig). Those deviated from the experimental assessment of the fitness benefit of the novel allele:  $s = 0.087 \pm 0.016$  for the polyploid replicon ( $n_{rc} = 15$ ) and  $s = 0.136 \pm 0.010$  for the monoploid replicon ( $n_{rc} = 1$ ) (see S8 Fig).

To examine how well our model captures the experimental results, we first performed simulations that correspond to the experimental conditions (Fig 3). The dynamics of the novel phenotype (kanamycin resistance) were overall in agreement with the results of the evolution experiment for both replicon types, albeit the frequency of the novel phenotype is slightly overestimated by the model given low or moderate initial frequencies ( $f_0 = 10^{-6}$  or  $10^{-7}$ ) or strong bottlenecks,  $b = 10^{-3}$ . The simulation results for the polyploid replicon show that the rise in frequency of heterozygotes in the experiment is well captured by the model simulations for high and moderate initial frequencies ( $f_0 = 10^{-4}$  and  $10^{-6}$ ) and bottleneck size combinations. Nonetheless, the model underestimates the frequency of heterozygotes observed in the evolution experiment, which is consistent with the overestimation of the loss rate of heterozygotes under neutral conditions. The frequency of heterozygotes in the simulation starts decaying at nearly the same transfer as in the experiment, yet heterozygotes in the evolution experiment reach frequencies that are 10- to 100-fold higher in comparison to the simulations. Note that a comparison of the simulated allele dynamics to the plasmid experiment for the low initial frequency ( $f_0 = 10^{-7}$ ) is not possible, as most replicates in those experiments went extinct. Using the model simulation for the low initial frequency thus supplies a theoretical expectation for the beneficial allele dynamics in rare cases where the novel allele may persist in the population. The simulation results for moderate and low initial frequencies ( $f_0 = 10^{-6}$  and  $10^{-7}$ ) predict a higher variability in the kanamycin-resistant cell frequencies per transfer for the polyploid replicon in comparison to the monoploid replicon (Fig 3A, plots 5–12). This prediction conforms to the results of the evolution experiments (S9 Fig). To further test the robustness of the comparison between theory and simulations regarding the choice of the parameter  $s$  in the model, we further performed computer simulations with  $s = 0.1$ . The resulting dynamics were qualitatively in agreement with our previous results as well (S10 Fig). We further compared the survival probability of the novel allele over time with the experimental results for the fraction of populations in which the allele is still present after a given transfer (Fig 3B). The model showed a remarkable agreement with the experimental results, capturing the main trends and often even making quantitatively accurate predictions.

### The establishment probability of alleles on polyploid replicons depends on the strength of selection and the replicon copy number

So far, we simulated polyploid replicons with a copy number and a selection coefficient that reflect the pTAD plasmid copy number and the beneficial effect of the *nptII* allele. To further examine the influence of the replicon ploidy level on the survival of novel beneficial alleles, we performed simulations for a range of replicon copy numbers and selection coefficients. The simulation results show that the establishment probability of a beneficial allele present in a single copy in a single cell,  $p_{\text{est}}$ , decreases with the replicon copy number (Fig 4), as previously found in a fully stochastic model without bottlenecks [27]. The strength of selection,  $s^{(50\%)}$ , required for equal chances of allele loss and allele establishment,  $p_{\text{est}} = 50\%$ , rises substantially within the range of copy numbers smaller than 5 and reaches a plateau for intermediate to high copy numbers. For the stronger bottlenecks,  $b = 10^{-3}$ , the threshold  $s^{(50\%)}$  is higher than for the weak bottleneck ( $b = 10^{-2}$ ), but the functional form with respect to the influence of the replicon copy number,  $n_{\text{rc}}$ , on  $s^{(50\%)}$  is qualitatively the same (Fig 4). For the weak bottleneck, the model predicts an  $s^{(50\%)}$  of ca. 20%, while for the strong bottlenecks, it is ca. 45% for copy numbers in the range between 10 and 20. Our model simulations thus demonstrate that the effect of replicon ploidy on the establishment probability of beneficial alleles is particularly pronounced at low replicon numbers. Copy numbers in the range of 1 to 10 are frequently observed in broad host range plasmids and is also typically reached by chromosomes of



**Fig 3. Model simulations of beneficial allele dynamics for polyploid ( $n_{rc} = 15$ ) and monoploid replicons.** Predicted frequencies of the novel phenotype, given has not (yet) gone extinct, are shown in (A) and the corresponding survival of the novel allele are shown in (B). (A) Cell frequencies of the novel phenotype (parallel to kanamycin-resistant cells) (black) and heterozygous cells (green) at the end of each population transfer obtained from 100 simulations for a replicon with copy number  $n_{rc} = 15$  (1,3,5,7,9,11, for the multicopy plasmid) and with  $n_{rc} = 1$  (2,4,6,8,10,12, reflecting the chromosome). Lines show the mean of positive frequencies over the number of transfers, i.e., the average proportion of cells having the novel phenotype from all simulation trajectories, where the novel allele has not (yet) gone extinct (cf. (B) for the survival of the allele). The initial population at the start of the first transfer consists of ancestral cells and a small proportion,  $f$ , of cells with one novel replicon copy, where  $f_0 = 10^{-4}$  in (1–4),  $f_0 = 10^{-6}$  in (5–8), and  $f_0 = 10^{-7}$  in (8–12). The grey (dark grey) areas show the 99% (67%) confidence intervals of positive frequencies of the novel phenotype. The green lines show the mean frequency of heterozygous cells

carrying both the ancestral and novel plasmid allele (conditioned on positive frequencies). Grey and green markers show the frequencies of kanamycin-resistant cells and heterozygous cells, respectively, of the corresponding experimental replicates. (B) Survival of the novel allele over number of transfers in model simulations (lines) and in the evolution experiment (markers)  $f_0 = 10^{-7}$ . The survival of the novel allele initially present at high initial frequencies,  $f_0 = 10^{-4}$ , are not shown since it is always 100%. The fraction of kanamycin-resistant cells of 100 simulation trajectories and 6 experimental replicates, respectively, is shown for each parameter combination. Simulation results were obtained by integrating Eq (1) with  $s = 0.087$  for the polyploid replicon and  $s = 0.136$  for the monoploid replicon until the population size has reached  $N_c(t)$  cells in each growth phase (transfer), where  $N_c(t)$  is taken from the mean experimental carrying capacity of each transfer  $t$ . A population bottleneck is applied after each growth phase, where a proportion of  $b = 10^{-2}$  or  $b = 10^{-3}$  cells are randomly selected from a multinomial distribution defined by the genotype frequencies at the end of the growth phase.

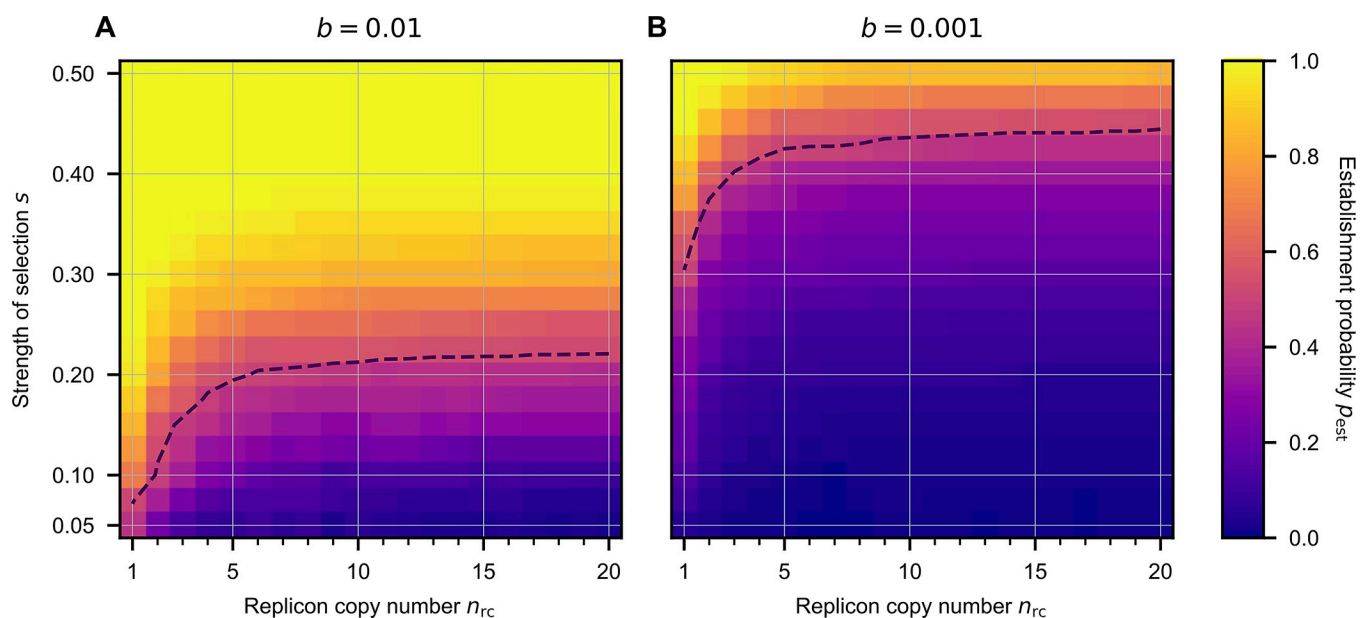
<https://doi.org/10.1371/journal.pgen.1010829.g003>

polyploid bacteria and of seemingly monoploid organisms during their growth phase (e.g., *E. coli* refs. [16,26,31]).

## Discussion

Polyploidy allows for the coexistence of multiple alleles on a replicon–chromosome or plasmid–within a single cell, thereby creating intracellular genetic diversity. The establishment of alleles encoded in polyploid replicons is thus affected by drift and selection at two hierarchical levels: the collective of replicons within a cell and the collective of cells within the population. Intracellular processes–replication and segregation–generate an effect of stochasticity that ultimately increases genetic drift and interferes with the establishment of novel alleles.

A key aspect influencing the dynamics of novel alleles in polyploid replicons is the mode of their replication and its coordination with cell division [9,29,32]. Regular replication is a deterministic mode of replication, where each replicon copy is duplicated exactly once prior to cell division. In contrast, in random replication, replicon copies are randomly selected for



**Fig 4. The influence of the replicon copy number ( $n_{rc}$ ) and the strength of selection ( $s$ ) on the establishment probability of a beneficial allele.** Allele establishment is achieved if the subpopulation of cells with the novel phenotype is sufficiently large, such that stochastic loss of the allele becomes unlikely. The dashed line shows the strength of selection  $s^{(50\%)}$  that is needed for a given replicon copy number,  $n_{rc}$ , to yield an establishment probability of 50%. Allele establishment in the simulation is defined by the time point when the frequency of novel homozygotes at the end of a growth phase (before a bottleneck) is sufficiently high such that the probability of allele extinction is below  $10^{-4}$ . The initial population consists of  $10^7$  cells, where one cell has a single mutant replicon copy and the rest is of the wild-type. The cell population grows until a carrying capacity  $N_c = 10^9$  before a population bottleneck occurs, where a fraction  $b = 10^{-2}$  or  $b = 10^{-3}$  of cells is transferred to form the new population in the next growth phase. Simulations stop either when the novel allele goes extinct or when the allele is established in the population.

<https://doi.org/10.1371/journal.pgen.1010829.g004>

replication throughout the cell growth cycle [33]. Using the regular replication mode, our model yielded accurate predictions of allele segregation rates and the decrease in heterozygote frequency in the early phase of the evolution experiment under non-selective conditions. Nonetheless, predictions for the allele dynamics overestimate the heterozygote loss rate as well as the mutant homozygote frequency under selective conditions. One possibility for the overestimated heterozygous loss rate could be a transient increase in the plasmid copy number during the evolution experiment. A further reason for deviations between theoretical and experimental results could be the choice of initial conditions in the simulations. The assumption of a single mutant replicon copy per cell is likely not strictly fulfilled. Moreover, the model ignores stochasticity in cell replication and death, and bottlenecks are the only source of stochasticity.

Employing our mathematical model, we deduce that our model plasmid pTAD-R may have a regular mode of replication. Notably, an experimental determination of the replication mode is a laborious endeavour, and only a few studies supplied a characterisation of specific replicons, including plasmids [34–36] and chromosomes [37]. Our study thus presents a potential novel approach for the inference of replication mode using a combination of experimentally determined and mathematically modelled allele dynamics, which could be applied to other replicons.

Rare alleles are subject to a high risk of stochastic loss, which was predicted early on by Haldane's theoretical result on the establishment probability,  $2s$ , for mutations encoded in monoploid replicons under selection of strength  $s$  (assuming a Poisson offspring number) [1]. For polyploid replicons, the presence of intracellular genetic diversity creates a subpopulation structure that can affect the establishment process of novel alleles. In our setup, the novel allele is initially introduced in a single copy out of  $n_{rc} = 15$  replicons within the cell. Loss of the novel allele is highly unlikely once the kanamycin-resistant cells reach a sufficiently high frequency in the population, as in the results of our high initial frequency scenario ( $10^{-4}$ ) under selection. However, novel alleles emerging via *de novo* mutations or recombination are expected to have a lower initial frequency (similar to our experimental frequencies  $10^{-6}$  and  $10^{-7}$ ). The establishment of such rare alleles would require an escape from stochastic loss in order to rise to high frequencies. Establishment is hindered in polyploid replicons since segregational drift generates homozygous cells and thus reduces the number of cells carrying the novel allele, thereby increasing stochastic effects in the cell dynamics. If daughter cells were exact copies of the mother cell, each inheriting one copy of the plasmid carrying the novel allele, establishment would be as likely as for alleles in monoploid replicons despite the lower initial allele frequency. At the same time, the mutational supply is higher in polyploid replicons [21], which may outweigh the effect of segregational drift, depending on the degree of dominance of beneficial alleles [27]. Whether for the same initial allele frequency (i.e., a higher absolute number of allele copies for the polyploid than for the monoploid replicon), loss is more likely on either replicon type depends also on the initial distribution of copies of the novel allele across cells: previous theoretical results for dominant alleles imply that loss would be less likely on the polyploid replicon if all cells carry only one copy of the novel allele initially [27]. In contrast, if all cells carrying the novel allele would be homozygous from the start, loss rates would be equal for both replicon types. Our current results show that rare beneficial alleles are more prone to stochastic loss and rise to fixation more slowly if the allele is present on a multicopy replicon (i.e., the pTAD-R plasmid) compared to alleles on a single-copy replicon (i.e., *A. baylyi* chromosome). A comparison of the experimental and mathematical results confirms that theory on establishment probabilities, as approximated by survival probabilities (starting from low initial frequencies), is highly suitable to capture and predict the empirical observations.

Comparing the effects of the selection regime and the replicon copy number in our theoretical model, we found that the minimal strength of selection to reach an establishment

probability of 50% ( $p_{\text{est}} = 50\%$ ) increases with the replicon copy number. The establishment probability  $p_{\text{est}}$  is most sensitive to the replicon copy number in a range of 1–10 copies per cell, which coincides with the copy number range of common polyploid chromosomes and natural plasmids. The effect of the replicon copy number has special significance in the context of antibiotic resistance evolution. Sub-inhibitory concentrations of antibiotics, like the ones employed in our experiment and simulations, are relevant for the emergence of resistant strains in natural environments and clinical settings, where the appearance of resistant mutants has been documented also under sub-inhibitory antibiotic exposure [38–40]. Our results suggest that novel antibiotic resistance variants will follow different evolutionary trajectories depending on the type of replicon where they emerge, i.e., chromosomes, low copy number plasmids or medium to high copy number plasmids. We hypothesise that the dependency of the establishment probability on the replicon copy number has an impact on the distribution of fitness effects of resistance mutations that reach fixation. Our results show that the establishment probability of beneficial alleles is negatively associated with the replicon copy number (at least up to ca.  $n_{\text{rc}} = 10$ ; see Fig 4), hence we expect that beneficial alleles in polyploid replicons require stronger selection to reach fixation compared to alleles in monoploid replicons. In other words, applying drug doses that lead to rapid fixation of resistance alleles in monoploid replicons, may result in loss of the resistance allele when the allele is encoded in a polyploid replicon. Taken together, segregational drift has an effect on the evolutionary rate of polyploid replicons by influencing the dynamics of beneficial alleles, from their emergence to their eventual loss or fixation.

## Materials and methods

### Bacterial strains, plasmids and culture conditions

The *A. baylyi* strain BD413 (DSM No. 588, German Collection of Microorganisms and Cell Cultures, DSMZ) also known as strain ADP1 (GenBank accession no. NC\_005966.1) was used as the model organism in all experiments. *A. baylyi* is a monoploid species with a single copy of its chromosome [41,42]. For the chromosomal allele experiments, *A. baylyi* strain BD4 was also used. Either *A. baylyi* BD413 or BD4 were used during plasmid or chromosomal modification constructions. Primers used in this study are listed in supplementary tables (S1 Table).

*A. baylyi* was propagated at 30 °C in LB medium in liquid shaking cultures or plates. For molecular cloning and plating, growth limiting factors, such as antibiotics, for the selection of plasmid/mutation carrying cells were used at the following concentrations: kanamycin 10 µg per ml, tetracycline 5 µg per ml, sucrose 50g per l. IPTG (Isopropyl β-D-1-thiogalactopyranoside) was added to the media to a final concentration of 1 mM when derepression of the LacI-repressed *pTrc* promoter was desired. Plasmids were extracted using the GeneJET Plasmid Miniprep Kit (Thermo Fisher Scientific). DNA quantification was done using the Multiskan GO spectrophotometer instrument (Thermo Fisher Scientific). All construction steps were validated by either restriction enzyme digestion or Sanger sequencing. The proof-reading Phusion polymerase (Thermo Scientific) was used for all PCR-based cloning.

The model plasmid pTAD employed in this study was constructed previously [28]. pTAD-R was introduced into a naïve *A. baylyi* strain BD413 (ADP1), where it is stably maintained due to a toxin-antitoxin system ( $0 \pm 0\%$  loss;  $n = 4$ ). The *A. baylyi* strains containing the chromosomal alleles were constructed via natural transformation followed by homologous recombination between an allele containing PCR product and the chromosome. The antibiotic resistance alleles were introduced independently in two *A. baylyi* strains in the same genomic region, the *alkM* gene (ACIAD\_RS06515). The kanamycin resistance allele (*nptII*) was inserted in the chromosome of *A. baylyi* BD413 strain (auxotrophic for tryptophan). The kanamycin resistance ancestral allele (*tetA*) encoding a tetracycline efflux protein, was inserted in the

chromosome of *A. baylyi* BD4 (tryptophan prototroph wild-type). The construction of the PCR product was done by SOEing PCR [43]. Two homologous regions to the *A. baylyi* chromosome flank the antibiotic resistance gene and were amplified by primer pairs (alkM-1up-fw/alkM\_2up-rv+o1) and (alkM\_5down-fw+o2/alkM\_6down-rv). The *sacB-nptII* was amplified from the gene targeting vector system pGT41 [44] using primer pair (sacB-fw+o1/nptII-rv+o2). The *tetA* gene was amplified from plasmid pRKNH3-ΔI a RK2 derivative [45] employing primer pair (ptetA\_tetA\_fw+o1/tetA\_rv+o2). The two fragments containing the homologous regions to the *A. baylyi* chromosome were joined in a SOEing PCR reaction with each antibiotic resistance gene, either *tetA* or *sacB-nptII*, independently.

### Fitness experiments

The relative fitness ( $w$ ) of the ancestral allele carrying strain versus the novel allele carrying strain was estimated by direct pairwise competition experiments, with 8 replicate populations for the plasmid replicon and 6 replicate populations for the chromosomal replicon. The determination of the selective coefficient given by the selection treatment was calculated via determination of the relative fitness of the ancestral allele carrying strain versus the novel allele carrying strain in direct pairwise competition experiments under selective conditions with 6 replicates populations for both plasmid and chromosomal replicons. The relative fitness ( $w$ ) of the ancestral kanamycin-resistant populations at the beginning of the experiment vs the evolved kanamycin-sensitive populations at the end of the experiment was estimated by direct pairwise competition experiments with 8 replicate populations per experimental condition tested (conditions 8 and 12). All competition experiments were initiated with a 1:1 ratio of the competing strains, diluted 1:100 from overnight cultures, pre-conditioned to growth in liquid media for two days. The relative fitness is calculated by calculating the growth of each of the competitors after 24 hours of growth, the cultures are serially transferred for 5 days and the populations determined. Serial transfer was done in non-selective media for ancestral carrying vs novel allele carrying population competition and on selective media (kanamycin 0.375 μg/ml) for selective coefficient determination and kanamycin-resistant vs non-resistant competition. The two competitors are distinguished by plating on non-selective (LB supplemented with IPTG 1mM) and selective media (LB supplemented with kanamycin 10 μg/ml for novel allele carrying strains (chromosome or plasmid) or M9 for ancestral allele carrying chromosomal strains).

### Natural transformation of *Acinetobacter baylyi*

The preparation of competent cells of *A. baylyi* carrying pTAD-R was prepared as described previously in ref. [45]. Briefly, the cells were grown at 30°C overnight with shaking in 2 ml of LB medium and used for the inoculation (1:100) of fresh cultures. These cultures were grown until early stationary phase (approx.  $1 \times 10^9$  cells per ml), cooled down and then stored as concentrated stocks ( $1 \times 10^{10}$  cell per ml) at -80°C.

For each transformation performed in the study, the frozen competent cells were thawed on ice and diluted to a cell density of  $2.5 \times 10^8$  cells per ml. The donor DNA was a PCR fragment (for a detailed description see ref. [28]) containing the non-disrupted *nptII*<sup>+</sup> as the single segment of sequence identity to the recipient plasmid. After 90 minutes of incubation at 30°C with shaking, diluted aliquots of the culture were plated on LB medium to estimate the titer of the population and transformants were scored on selective media. Transformation frequencies were calculated as transformants per recipient.

Natural transformation in *A. baylyi* follows one-hit kinetics [46], where the number of created transformants is proportional to the concentration of donor DNA added in the transformation process. The uptake probability of DNA molecules per host cell does not change with

increasing concentration of DNA. Therefore a single donor DNA molecule recombines with the host DNA in the vast majority of cells (97% [28]).

## Evolution experiments

The plasmid allele dynamics evolution experiment was conducted with ancestral plasmid carrying *A. baylyi* populations under two selection regimes, three novel initial allele frequencies and two population bottleneck sizes. The ancestral plasmid present was pTAD-R for all populations ( $n = 72$ ). On the onset of the experiment, *A. baylyi* strain BD413 containing the ancestral plasmid was naturally transformed with the donor DNA as explained in the previous section following the previously described protocol [28]. Donor DNA was added at specific concentrations to generate diverse transformants frequencies. Three different initial allele frequencies were created:  $10^{-4}$  (700ng/ml donor DNA),  $10^{-6}$  (7ng/ml donor DNA) and  $10^{-7}$  (0.7ng/ml donor DNA). After the transformation was complete (i.e., after 90 minutes of incubation), a fraction of the cells was plated to determine the total cell population and the transformation frequency. The viable titer of the cultures was obtained from the cells plated on LB media ( $10^{-4}$ ,  $10^{-5}$  and  $10^{-6}$  dilutions), whereas the transformation efficiency was calculated by plating on LB + kanamycin (5  $\mu\text{g/ml}$ ) (1,  $10^{-1}$  and  $10^{-2}$  dilutions). Cells that had restored the *nptII* gene on one of copies of the recipient plasmid survived the kanamycin treatment. After overnight growth cultures were diluted into fresh medium with 1:100 (weak bottleneck) or 1:1000 (strong bottleneck) dilution factor. The bacterial populations were subjected to two selective regimes, non-selective conditions and selective conditions (kanamycin 0.375  $\mu\text{g/ml}$ ). The cultures were incubated in 96-deep-well plates with a total volume of 1 ml at 30°C with constant shaking. The transfer regime was then maintained for 30 transfers, which corresponds to approx. 200–300 generations (~6–7 generations per transfer in liquid medium for the weak bottleneck and ~9–10 generations for the strong bottleneck). Every day the population sizes were estimated, the total population size was estimated from the plating on LB media and the proportion of hosts in the population was measured by plating on selective media, LB supplemented with kanamycin. The distinction between heterozygotes and homozygotes for the new allele (*nptII*) comes from the gene of the reporter construct. For our model plasmid, the fluorescence that confers the GFP protein enables us to distinguish them.

The chromosomal allele experiment was performed by employing a mixture of two *A. baylyi* strains, BD4 (tryptophan prototroph) carrying a *tetA* gene which is the ancestral allele in this setting and BD413 (tryptophan auxotroph) carrying a *nptII* gene which is the novel allele. The strains were then mixed in three ratios comparable to the initial novel allele frequencies of the plasmid experiment, BD4/BD413 at  $10^{-4}$ ,  $10^{-6}$  and  $10^{-7}$  proportions. A fraction of the cell was plated to determine the initial host proportion and the cell titers were calculated as previously described employing M9 minimal media and LB supplemented with kanamycin (5  $\mu\text{g/ml}$ ) as selective media to distinguish both strains. The experimental set up was identical as the one employed for the plasmid allele dynamics experiment, with serially passaged populations employing a 1:100 or 1:1000 dilution factor under non-selective and selective conditions ( $n = 72$ ). The bacterial populations were subjected to two selective regimes, non-selective conditions and selective conditions (kanamycin 0.4  $\mu\text{g/ml}$ ). The cultures were transferred for 30 transfers and population size estimation was done for each day.

## Statistical analysis

All statistical tests and data analysis were performed in RStudio version 1.2.1327. Comparisons between groups (e.g., fitness calculations) were performed with two sided Wilcoxon signed-rank test [47] by the “wilcox.test” function.



### Simulation

We simulate the population dynamics of the serial dilution experiment using a random segregation model for multicopy replicons [27,29], which we extended for periodic bottlenecks. The model comprises competitive growth of bacteria, periodic bottlenecks, and plasmid segregation. In our model, cells with at least one copy ( $i \geq 1$ ) of the novel (resistance-conferring) plasmid variant have an intrinsic cell division rate  $r_i = 1$ , where  $i$  denotes the cell type. Bacteria without the novel plasmid variant have an intrinsic cell division rate  $r_0 = 1 - s$ , where  $s > 0$  reflecting an antibiotic environment or  $s = 0$  for a neutral environment. We ignore cell death. At the beginning of the simulation, the population consists of  $N^{(0)} = 10^7$  cells with a (resistant) sub-population of proportion  $f_0$  that carries one (out of  $n_{rc}$ ) replicon copy of the novel variant. All cells have a fixed copy number of the plasmid  $n_{rc}$  at cell birth. We describe two modes of plasmid replication during cell division, regular and random replication. For regular replication, all plasmid copies are duplicated in a parental cell before it divides. For random replication, plasmid replication follows a successive manner. First, one plasmid is randomly chosen from the plasmid pool for replication and the two replicates are added to the pool of plasmids (see also [33]). This procedure is repeated  $n_{rc} - 1$  more times such that a cell—as for regular replication—carries  $2n_{rc}$  plasmid copies before cell division. Finally, plasmid copies are distributed to the bacterial daughter cells at random, but in equal numbers to comply with the fixed plasmid copy number  $n_{rc}$  [cf. 27,29]. The influence of the assumption of fixed copy numbers on rescue probabilities (and thus indirectly establishment probabilities) on multicopy plasmids was discussed previously and shown to be small, especially for dominant mutations [27]. Bacterial populations grow logistically up to a carrying capacity  $\hat{N}^{(B)}$  before the transfer (bottleneck)  $B$  occurs, which we determine separately for each individual transfer and condition as the mean over the six experimental replicates. We model population growth between bottlenecks deterministically, which is much faster to simulate than a fully stochastic model. This model implementation is based on the assumption that bottlenecks (see below) are the dominating source of stochasticity. We, thus, have a system of  $n_{rc} + 1$  differential equations that describe the temporal change of the cell numbers  $N_i$  for the individual cell types  $i = 0, \dots, n_{rc}$  (cells carrying  $i$  novel plasmid copies) between two bottlenecks,  $B-1$  and  $B$ .

Cells of any type  $j$  divide at a rate  $r_j \left( 1 - \frac{\sum_{i=0}^{n_{rc}} N_i}{\hat{N}^{(B)}} \right)$ . We thus obtain

$$\dot{N}_i = \sum_{j=0}^{n_{rc}} r_j N_j \left( m_{j \rightarrow i} - \delta_{ij} \right) \left( 1 - \frac{\sum_{i=0}^{n_{rc}} N_i}{\hat{N}^{(B)}} \right) \tag{1}$$

where  $m_{j \rightarrow i}$  denotes the expected number of  $i$ -type cells produced at division of an  $j$ -type cell. Kronecker's delta ( $\delta_{ij} = 1$  for  $i = j$  and 0 otherwise) takes into account that the mother cell is replaced by two daughter cells at cell division.

For the expressions for  $m_{j \rightarrow i}$  for regular and random replication, we refer to Appendix A in [29].

We define the end of the growth phase by the time when the time derivative of the various cell numbers,  $N_i$ , becomes very low,  $|\dot{N}_i| \leq 0.01$  for all cell types  $i$ , i.e., the change in the cell number of any cell type is at maximum 1% of the per-capita growth rate of wild-type cells. At this time, the carrying capacity is almost reached as the change in the total cell number  $\sum_{i=0}^{n_{rc}} \dot{N}_i < 0.01 n_{rc}$  becomes very low. With this implementation, the number of cell divisions between bottlenecks in the simulations is expected to be similar to that in the experiments. At the end of the growth phase, populations undergo a bottleneck of factor  $b$ , which we model stochastically by drawing a proportion  $b$  of the population at carrying capacity (rounded to an

integer number) using a multinomial distribution generated by the proportions of all cell types  $i$  in the population.

### Estimation of model parameter of selection $s$

We used optimization methods to estimate the model parameter  $s$  from the time series of kanamycin-resistant cell frequencies. Optimal  $s$  values were obtained by performing a nonlinear least-square analysis with the residuals

$$e_B = \frac{\log \hat{N}_{res}^{(sim,B)}(s) - \langle \log \hat{N}_{res}^{(exp,B)} \rangle}{\sigma_B}$$

where  $\hat{N}_{res}^{(sim,B)}(s) = \sum_{i=1}^{n_{rc}} \hat{N}_i^{(sim,B)}(s)$  and  $\hat{N}_{res}^{(exp,B)} = \sum_{i=1}^{n_{rc}} \hat{N}_i^{(exp,B)}$  denote the resistant cell frequencies before transfer  $B$  in computer simulations for a given parameter  $s$  and in the experiment respectively [48]. The standard deviations of logarithmic resistant cell frequencies in the experiment at transfer  $B$  is denoted by  $\sigma_B$ . We transformed simulation and experimental data using a logarithmic scale because of the exponential growth in our model (see Eq (1)). The experimental data was averaged over the six experimental replicates indicated by the angle brackets in the latter equation. We use the conditions with high initial frequencies  $f_0 = 10^{-4}$  and weak bottlenecks  $b = 10^{-2}$  for the parameter estimation to minimize the stochasticity from population bottlenecks. For the computer simulation, we use only single trajectories for the optimization due to the low variability under these conditions (see Fig 3A, plot 1 and 3). The nonlinear regression to estimate  $s$  was performed using least-squares minimization methods implemented in the Python package *lmfit* (function *minimize*, parameter *method* = 'least\_squares'). The minimization of the residuals was initiated at  $s = 0.1$ .

## Supporting information

**S1 Fig. Comparison between the allele dynamics in evolution experiments using the pTAD-R plasmid and in model simulations.** Simulations with (A) different replicon copy numbers  $n_{rc}$  (see legend) under non-selective conditions ( $s = 0$ ) and with (B)  $n_{rc} = 15$  and different negative selection parameters  $s < 0$ . Simulations and experiments were performed with high initial frequencies,  $f_0 = 10^{-4}$ , and weak bottlenecks,  $b = 10^{-2}$ . Bold green (red) lines show the median of the heterozygote (homozygote) frequencies before each transfer from 10 simulations for each replicon copy number. Thin lines show the heterozygote frequency from the six replicates of the evolution experiment. Simulation results were obtained as described for Fig 1D. (TIF)

**S2 Fig. Competition experiments to quantify the fitness differences between the ancestral and novel alleles homozygotes.** a) Pairwise competition experiments between plasmid carrying strains *A. baylyi* BD413 pTAD-R (*GFP*, ancestral plasmid allele) and *A. baylyi* BD413 pTAD-R (*nptIII*, novel plasmid allele); *A. baylyi* BD4 (*tetA*, ancestral chromosome allele) and *A. baylyi* BD413 (*nptIII*, novel chromosomal allele). The experiments were conducted under non-selective conditions employing a transfer regime where cultures were grown at 30°C and serially passaged every 24h for a duration of 120h. Experiments were conducted with 6 biological replicates per replicon. Fitness was calculated relative to the growth as described in refs. [50,51], no significant fitness effect could be observed (pTAD-R  $H_0: w = 1$ ,  $p = 0.4375$ ,  $n = 6$  & Chromosome  $H_0: w = 1$ ,  $p = 0.0625$ ,  $n = 6$ . Wilcoxon test). b) Selection coefficient applicable to the ancestral allele carrying strain under non-selective conditions. Selection coefficient was calculated by the formula  $s = w - 1$  [50]. No significant selection coefficient was applicable to

any strain.  
(TIFF)

**S3 Fig. Plasmid allele dynamics in nonselective and selective conditions under weak bottleneck (1:100 or  $10^{-2}$ ).** (A) The dynamics of pTAD-R over approximately 200 generations. The novel allele was introduced at the beginning of the experiment employing different donor DNA concentration to achieve 3 initial allele frequencies. Host frequencies in the total population are shown in black, heterozygote frequencies are shown in green and novel homozygotes in pink. a) High initial frequencies b) Moderate initial frequencies c) Small initial frequencies. (TIFF)

**S4 Fig. Plasmid allele dynamics in nonselective and selective conditions under strong bottleneck (1:1000 or  $10^{-3}$ ).** (A) The dynamics of pTAD-R over approximately 200 generations. The novel allele was introduced at the beginning of the experiment employing different donor DNA concentration to achieve 3 initial allele frequencies. Host frequencies in the total population are shown in black, heterozygote frequencies are shown in green and novel homozygotes in pink. a) High initial frequencies b) Moderate initial frequencies c) Small initial frequencies. (TIFF)

**S5 Fig. Competition experiments to quantify the fitness differences between the ancestral and novel alleles homozygotes under selective conditions.** a) Pairwise competition experiments between plasmid carrying strains *A. baylyi* BD413 pTAD-R (*GFP*, ancestral plasmid allele) and *A. baylyi* BD413 pTAD-R (*nptII*, novel plasmid allele); *A. baylyi* BD4 (*tetA*, ancestral chromosomal allele) and *A. baylyi* BD413 (*nptII*, novel chromosomal allele). The experiments were conducted under selective conditions ( $\text{kanamycin}_{\text{plasmid}} = 0.375\mu\text{g/ml}$  and  $\text{kanamycin}_{\text{chromosome}} = 0.4\mu\text{g/ml}$ ) A bigger range of antibiotic concentrations were first tested for the plasmid replicon to determine the range of kanamycin concentrations that would give the desired selective benefit. The chromosomal antibiotic values tested were restricted to those closer to the plasmid replicon concentration values. A transfer regime was employed where cultures were grown at 30°C and serially passaged every 24h for a duration of 120h. Experiments were conducted with 6 biological replicates per replicon. Fitness was calculated relative to the growth as described in refs. [50,51], a lower fitness effect could be observed under selective conditions, where the fitness was not significantly different than 0.9 (pTAD-R  $H_0: w = 0.9$ ,  $p = 0.4375$ ,  $n = 6$  & Chromosome  $H_0: w = 0.9$ ,  $p = 0.5625$ ,  $n = 6$ . Wilcoxon test). b) Selection coefficient applicable to the ancestral allele carrying strain under selective conditions. Selection coefficient was calculated by the formula  $s = w - 1$  [50]. A significant selection coefficient was applicable to the ancestral strain. The antibiotic treatment applied to the plasmid gives a mean selective coefficient of  $s = -0.1185 \pm 0.0415$ , that was not significantly different from  $s = -0.1$  ( $p = 0.4375$ , using Wilcoxon test,  $n = 6$ ). For the chromosomal replicon the antibiotic treatment gives a mean selective coefficient of  $s = -0.0984 \pm 0.0305$ , with no significant difference from  $s = -0.1$  ( $p = 0.5625$ , using Wilcoxon test,  $n = 6$ ). Ancestral allele containing strain shows a selective disadvantage ( $s < 0$ ) of 0.1. (TIFF)

**S6 Fig. Competition experiments to quantify the fitness differences between the ancestral and novel alleles homozygotes under diverse selective conditions.** a) Pairwise competition experiments between plasmid carrying strains *A. baylyi* BD413 pTAD-R (*GFP*, ancestral plasmid allele) and *A. baylyi* BD413 pTAD-R (*nptII*, novel plasmid allele); *A. baylyi* BD4 (*tetA*, ancestral chromosomal allele) and *A. baylyi* BD413 (*nptII*, novel chromosomal allele). The experiments were conducted under diverse selective conditions ( $\text{kanamycin}_{\text{plasmid}} = 0.1-1.5\mu\text{g/ml}$  and  $\text{kanamycin}_{\text{chromosome}} = 0.375\&0.4\mu\text{g/ml}$ ) employing a transfer regime where

cultures were grown at 30°C and serially passaged every 24h for a duration of 120h. Experiments were conducted with 4–6 biological replicates per kanamycin concentration assayed. Fitness was calculated relative to the growth as described in refs. [50,51]. Selection coefficient applicable to the ancestral allele carrying strain under selective conditions. Selection coefficient was calculated by the formula  $s = w - 1$  [50].

(TIFF)

**S7 Fig. Quantification of fitness differences under selective conditions between the evolved kanamycin-sensitive populations of the end of the experiment and the ancestral kanamycin-resistant populations of the beginning of the experiment.** Pairwise competition experiments between evolved kanamycin-sensitive and ancestral kanamycin-resistant populations of experimental conditions 8 and 12. The experiments were conducted in selective medium (kanamycin 0.375 µg/ml) employing a transfer regime where cultures were grown at 30°C and serially passaged every 24h for a duration of 120h. Experiments were conducted with 8 biological replicates per condition. Fitness was calculated relative to the growth as described in refs. [50,51]. A significant fitness disadvantage of the kanamycin-sensitive population could be observed (Cond 8  $H_0: w > 1$ ,  $p = 0.003906$ ,  $n = 8$  & Cond 12  $H_0: w > 1$ ,  $p = 0.007813$ ,  $n = 8$ ). Data also shows a fitness advantage of the kanamycin-resistant over the kanamycin-sensitive population with a selection coefficient of 0.1 for the kanamycin-sensitive (Cond 8  $H_0: w = 0.9$ ,  $p = 0.25$ ,  $n = 8$  & Cond 12  $H_0: w = 0.9$ ,  $p = 0.1484$ ,  $n = 8$ ).

(TIFF)

**S8 Fig. Goodness of fit for the estimated  $s$  values of the simulated allele dynamics.** a) The regression standard error,  $\sqrt{\chi^2/\nu} = \sqrt{\sum_{B=1}^{30} e_B^2/\nu}$  where  $\chi^2 = \sum_{B=1}^{30} e_B^2$  (weighted sum of squared deviations) and  $\nu = 30 - 1$  (degree of freedom), for the simulated allele dynamics on the polyploid replicon ( $n_{rc} = 15$ ) with different selection coefficients  $s$ , which yields an optimal fit to the experimental allele dynamics on the chromosome with  $s = 0.087 \pm 0.016$  (standard error). b) The simulated allele dynamics on the monoploid replicon ( $n_{rc} = 1$ ), which yields an optimal fit to the experimental allele dynamics on the multicopy plasmid with  $s = 0.136 \pm 0.010$ . We fitted the selection coefficients using the cell frequencies of the novel phenotype (kanamycin-resistant) for the experimental conditions  $f_0 = 10^{-4}$  and  $b = 0.01$ . Blue lines show the experimentally estimated selection coefficients. The minimization of the residuals was initiated at  $s = 0.1$  using standard least-square minimization methods (see text). The plots above show data points for the regression standard error additional to the  $s$  values reached by the minimization method. The boxes show the 95% confidence intervals of the estimated  $s$  values for the experimental  $s$  (blue) and the theoretical  $s$  (gray).

(TIFF)

**S9 Fig. Coefficient of variation of kanamycin-resistant cell proportion for high initial allele frequency populations ( $f_0 = 10^{-4}$ ).** Lines present the trendline and the shaded area corresponds to the confidence interval.

(TIFF)

**S10 Fig. Model simulations of beneficial allele dynamics for polyploid ( $n_{rc} = 15$ ) and monoploid replicons with a selection parameter  $s = 0.1$ .** Analogue to Fig 3, where we used  $s = 0.087$  ( $s = 0.136$ ) for the novel allele on the polyploid (monoploid) replicon, predicted frequencies of the novel phenotype are shown in (A) and the corresponding survival of the novel allele are shown in (B). (A) Cell frequencies of the novel phenotype (parallel to kanamycin-resistant cells) (black) and heterozygous cells (green) at the end of each population transfer obtained from 100 simulations for a replicon with copy number  $n_{rc} = 15$  (1,3,5,7,9,11; for the

multicopy plasmid) and with  $n_{rc} = 1$  (2,4,6,8,10,12; reflecting the chromosome). Lines show the mean of positive frequencies over the number of transfers, i.e., the average proportion of cells having the novel phenotype from all simulation trajectories, where the novel allele has not (yet) gone extinct (cf. (B) for the survival of the allele). The initial population at the start of the first transfer consists of ancestral cells and a small proportion,  $f$ , of cells with one novel replicon copy, where  $f_0 = 10^{-4}$  in (1–4),  $f_0 = 10^{-6}$  in (5–8), and  $f_0 = 10^{-7}$  in (8–12). The grey (dark grey) areas show the 99% (67%) confidence intervals of positive frequencies of the novel phenotype. The green lines show the mean frequency of heterozygous cells carrying both the ancestral and novel plasmid allele (conditioned on positive frequencies). Grey and green markers show the frequencies of kanamycin-resistant cells and heterozygous cells, respectively, of the corresponding experimental replicates. (B) Survival of the novel allele over number of transfers in model simulations (lines) and in the evolution experiment (markers) for intermediate initial frequencies,  $f_0 = 10^{-6}$ , (1–4) and low initial frequencies,  $f_0 = 10^{-7}$ . The survival of the novel allele initially present at high initial frequencies,  $f_0 = 10^{-4}$ , are not shown since it is always 100%. The fraction of kanamycin-resistant cells of 100 simulation trajectories and 6 experimental replicates, respectively, is shown for each parameter combination. Simulation results were obtained as described in the caption of Fig 3.

(TIFF)

#### **S1 Table. Primers used in the study.**

(XLSX)

#### **S1 Data. Source data underlying Figs 1, 2, S2, S5, S6 and S7.**

(XLSX)

## **Acknowledgments**

We thank Daniela Kluger and Ian Dewan for their assistance in the experimental work. The authors thank Yiqing Wang, Shreya Vichare and Ishan Bhatt for critical comments on the manuscript, the entire Genomic Microbiology group and Stochastic Evolutionary Dynamics group for their help and discussions.

## **Author Contributions**

**Conceptualization:** Ana Garoña, Mario Santer, Nils F. Hülter, Hildegard Uecker, Tal Dagan.

**Data curation:** Ana Garoña, Mario Santer.

**Formal analysis:** Ana Garoña, Mario Santer, Nils F. Hülter.

**Funding acquisition:** Hildegard Uecker, Tal Dagan.

**Investigation:** Ana Garoña, Mario Santer, Nils F. Hülter.

**Methodology:** Ana Garoña, Mario Santer, Nils F. Hülter.

**Software:** Mario Santer.

**Visualization:** Ana Garoña, Mario Santer.

**Writing – original draft:** Ana Garoña, Mario Santer.

**Writing – review & editing:** Ana Garoña, Mario Santer, Nils F. Hülter, Hildegard Uecker, Tal Dagan.

## References

1. Haldane JBS. A Mathematical Theory of Natural and Artificial Selection, Part V: Selection and Mutation. *Mathematical Proceedings of the Cambridge Philosophical Society*. 1927 Jul; 23(7):838–44.
2. Patwa Z, Wahl L m. The fixation probability of beneficial mutations. *Journal of The Royal Society Interface*. 2008 Nov 6; 5(28):1279–89. <https://doi.org/10.1098/rsif.2008.0248> PMID: 18664425
3. Wahl LM. Fixation when N and s Vary: Classic Approaches Give Elegant New Results. *Genetics*. 2011 Aug 1; 188(4):783–5. <https://doi.org/10.1534/genetics.111.131748> PMID: 21828279
4. Laxminarayan R, Duse A, Wattal C, Zaidi AKM, Wertheim HFL, Sumpradit N, et al. Antibiotic resistance—the need for global solutions. *The Lancet Infectious Diseases*. 2013 Dec 1; 13(12):1057–98. [https://doi.org/10.1016/S1473-3099\(13\)70318-9](https://doi.org/10.1016/S1473-3099(13)70318-9) PMID: 24252483
5. Carroll SP, Jørgensen PS, Kinnison MT, Bergstrom CT, Denison RF, Gluckman P, et al. Applying evolutionary biology to address global challenges. *Science*. 2014 Oct 17; 346(6207):1245993. <https://doi.org/10.1126/science.1245993> PMID: 25213376
6. Alexander HK, MacLean RC. Stochastic bacterial population dynamics restrict the establishment of antibiotic resistance from single cells. *Proc Natl Acad Sci USA*. 2020 Jul 23;201919672. <https://doi.org/10.1073/pnas.1919672117> PMID: 32703812
7. Saebelfeld M, Das SG, Hagenbeek A, Krug J, de Visser JAGM. Stochastic establishment of  $\beta$ -lactam-resistant *Escherichia coli* mutants reveals conditions for collective resistance. *Proceedings of the Royal Society B: Biological Sciences*. 2022 May 11; 289(1974):20212486.
8. Saebelfeld M, Das SG, Brink J, Hagenbeek A, Krug J, de Visser JAGM. Antibiotic Breakdown by Susceptible Bacteria Enhances the Establishment of  $\beta$ -Lactam Resistant Mutants. *Frontiers in Microbiology* [Internet]. 2021 [cited 2022 Sep 25];12. Available from: <https://www.frontiersin.org/articles/10.3389/fmicb.2021.698970>.
9. Reyes-Lamothe R, Nicolas E, Sherratt DJ. Chromosome Replication and Segregation in Bacteria. *Annual Review of Genetics*. 2012; 46(1):121–43. <https://doi.org/10.1146/annurev-genet-110711-155421> PMID: 22934648
10. Watanabe S. Cyanobacterial multi-copy chromosomes and their replication. *Bioscience, Biotechnology, and Biochemistry*. 2020 Jul 2; 84(7):1309–21. <https://doi.org/10.1080/09168451.2020.1736983> PMID: 32157949
11. Mori T, Binder B, Johnson CH. Circadian gating of cell division in cyanobacteria growing with average doubling times of less than 24 hours. *Proceedings of the National Academy of Sciences*. 1996 Sep 17; 93(19):10183–8. <https://doi.org/10.1073/pnas.93.19.10183> PMID: 8816773
12. Kitten T, Barbour AG. The relapsing fever agent *Borrelia hermsii* has multiple copies of its chromosome and linear plasmids. *Genetics*. 1992 Oct 1; 132(2):311–24. <https://doi.org/10.1093/genetics/132.2.311> PMID: 1427031
13. Maldonado R, Jiménez J, Casadesús J. Changes of ploidy during the *Azotobacter vinelandii* growth cycle. *Journal of Bacteriology*. 1994 Jul; 176(13):3911–9. <https://doi.org/10.1128/jb.176.13.3911-3919.1994> PMID: 8021173
14. Hildenbrand C, Stock T, Lange C, Rother M, Soppa J. Genome copy numbers and Gene Conversion in Methanogenic Archaea. *Journal of Bacteriology*. 2011 Feb; 193(3):734–43. <https://doi.org/10.1128/JB.01016-10> PMID: 21097629
15. Morse ML, Lederberg EM, Lederberg J. TRANSDUCTIONAL HETEROGENOTES IN *ESCHERICHIA COLI*. *Genetics*. 1956 Sep 1; 41(5):758–79. <https://doi.org/10.1093/genetics/41.5.758> PMID: 17247661
16. Nielsen HJ, Youngren B, Hansen FG, Austin S. Dynamics of *Escherichia coli* Chromosome Segregation during Multifork Replication. *Journal of Bacteriology*. 2007 Dec; 189(23):8660–6. <https://doi.org/10.1128/JB.01212-07> PMID: 17905986
17. Bazaal M, Helinski DR. Circular DNA forms of colicinogenic factors E1, E2 and E3 from *Escherichia coli*. *Journal of Molecular Biology*. 1968 Sep 14; 36(2):185–94. [https://doi.org/10.1016/0022-2836\(68\)90374-4](https://doi.org/10.1016/0022-2836(68)90374-4) PMID: 4939624
18. Projan SJ, Monod M, Narayanan CS, Dubnau D. Replication properties of pIM13, a naturally occurring plasmid found in *Bacillus subtilis*, and of its close relative pE5, a plasmid native to *Staphylococcus aureus*. *Journal of Bacteriology*. 1987; 169(11):5131–9. <https://doi.org/10.1128/jb.169.11.5131-5139.1987> PMID: 2822666
19. Lin-Chao S, Bremer H. Effect of the bacterial growth rate on replication control of plasmid pBR322 in *Escherichia coli*. *Mol Gen Genet*. 1986 Apr 1; 203(1):143–9. <https://doi.org/10.1007/BF00330395> PMID: 2423846
20. Węgrzyn G. Replication of Plasmids during Bacterial Response to Amino Acid Starvation. *Plasmid*. 1999 Jan 1; 41(1):1–16. <https://doi.org/10.1006/plas.1998.1377> PMID: 9887302

21. San Millan A, Escudero JA, Gifford DR, Mazel D, MacLean RC. Multicopy plasmids potentiate the evolution of antibiotic resistance in bacteria. *Nat Ecol Evol*. 2017 Jan; 1(1):0010.
22. Santos-Lopez A, Bernabe-Balas C, Ares-Arroyo M, Ortega-Huedo R, Hoefler A, Millan AS, et al. A Naturally Occurring Single Nucleotide Polymorphism in a Multicopy Plasmid Produces a Reversible Increase in Antibiotic Resistance. *Antimicrobial Agents and Chemotherapy*. 2017 Feb 1; 61(2):e01735–16. <https://doi.org/10.1128/AAC.01735-16> PMID: 27895020
23. Rodríguez-Beltrán J, Hernández-Beltrán JCR, DelaFuente J, Escudero JA, Fuentes-Hernández A, MacLean RC, et al. Multicopy plasmids allow bacteria to escape from fitness trade-offs during evolutionary innovation. *Nature Ecology & Evolution*. 2018 May; 2(5):873–81. <https://doi.org/10.1038/s41559-018-0529-z> PMID: 29632354
24. Soppa J. Non-equivalent genomes in polyploid prokaryotes. *Nat Microbiol*. 2022 Feb; 7(2):186–8. <https://doi.org/10.1038/s41564-021-01034-3> PMID: 34949829
25. Ilhan J, Kupczok A, Woehle C, Wein T, Hülter NF, Rosenstiel P, et al. Segregational Drift and the Interplay between Plasmid Copy Number and Evolvability. Falush D, editor. *Molecular Biology and Evolution*. 2019 Mar 1; 36(3):472–86. <https://doi.org/10.1093/molbev/msy225> PMID: 30517696
26. Sun L, Alexander HK, Bogos B, Kiviet DJ, Ackermann M, Bonhoeffer S. Effective polyploidy causes phenotypic delay and influences bacterial evolvability. *PLoS Biology*. 2018 Feb 22; 16(2):e2004644. <https://doi.org/10.1371/journal.pbio.2004644> PMID: 29470493
27. Santer M, Uecker H. Evolutionary Rescue and Drug Resistance on Multicopy Plasmids. *Genetics*. 2020 Jul 1; 215(3):847–68. <https://doi.org/10.1534/genetics.119.303012> PMID: 32461266
28. Garoña A, Hülter NF, Romero Picazo D, Dagan T. Segregational Drift Constrains the Evolutionary Rate of Prokaryotic Plasmids. *Molecular Biology and Evolution*. 2021 Dec 1; 38(12):5610–24. <https://doi.org/10.1093/molbev/msab283> PMID: 34550379
29. Santer M, Kupczok A, Dagan T, Uecker H. Fixation dynamics of beneficial alleles in prokaryotic polyploid chromosomes and plasmids. *Genetics*. 2022 222(2), iyac121. <https://doi.org/10.1093/genetics/iyac121> PMID: 35959975
30. Bodmer WF, Cavalli-Sforza LL. *Genetics, Evolution, and Man*. W.H.Freeman; 1976.
31. Akerlund T, Nordström K, Bernander R. Analysis of cell size and DNA content in exponentially growing and stationary-phase batch cultures of *Escherichia coli*. *Journal of Bacteriology*. 1995 Dec; 177(23):6791–7. <https://doi.org/10.1128/jb.177.23.6791-6797.1995> PMID: 7592469
32. Li H. Random Chromosome Partitioning in the Polyploid Bacterium *Thermus thermophilus* HB27. *G3*. 2019 Feb 21;g3.400086.2019. <https://doi.org/10.1534/g3.119.400086> PMID: 30792193
33. Novick RP, Hoppensteadt FC. On plasmid incompatibility. *Plasmid*. 1978 Sep; 1(4):421–34. [https://doi.org/10.1016/0147-619x\(78\)90001-x](https://doi.org/10.1016/0147-619x(78)90001-x) PMID: 372974
34. Rownd R. Replication of a Bacterial Episome under Relaxed control. *Journal of Molecular Biology*. 1969; 44:387–402. [https://doi.org/10.1016/0022-2836\(69\)90368-4](https://doi.org/10.1016/0022-2836(69)90368-4) PMID: 5346048
35. Bazaral MG, Helinski DR. Replication of a bacterial plasmid and an episome in *Escherichia coli*. *Biochemistry*. 1970 Jan 20; 9(2):399–406. <https://doi.org/10.1021/bi00804a029> PMID: 4904868
36. Gustafsson P, Nordström K. Random replication of the stringent plasmid R1 in *Escherichia coli* K-12. *Journal of Bacteriology*. 1975 Aug; 123(2):443–8. <https://doi.org/10.1128/jb.123.2.443-448.1975> PMID: 1097410
37. Skarstad K, Boye E, Steen HB. Timing of initiation of chromosome replication in individual *Escherichia coli* cells. *The EMBO Journal*. 1986 Jul; 5(7):1711–7. <https://doi.org/10.1002/j.1460-2075.1986.tb04415.x> PMID: 3527695
38. Sanz-García F, Hernando-Amado S, Martínez JL. Evolution under low antibiotic concentrations: a risk for the selection of *Pseudomonas aeruginosa* multidrug-resistant mutants in nature. *Environmental Microbiology*. 2022; 24(3):1279–93. <https://doi.org/10.1111/1462-2920.15806> PMID: 34666420
39. Wistrand-Yuen E, Knopp M, Hjort K, Koskiniemi S, Berg OG, Andersson DI. Evolution of high-level resistance during low-level antibiotic exposure. *Nat Commun*. 2018 Apr 23; 9(1):1599. <https://doi.org/10.1038/s41467-018-04059-1> PMID: 29686259
40. Pereira C, Warsi OM, Andersson DI. Pervasive Selection for Clinically Relevant Resistance and Media Adaptive Mutations at Very Low Antibiotic Concentrations. *Molecular Biology and Evolution*. 2023 Jan 1; 40(1):msad010. <https://doi.org/10.1093/molbev/msad010> PMID: 36627817
41. Cuff E. L. (2013). Genomic plasticity and chromosomal copy number of *Acinetobacter baylyi* ADP1 [Doctoral dissertation, University of Georgia] [http://getd.libs.uga.edu/pdfs/cuff\\_laura\\_e\\_201308\\_phd.pdf](http://getd.libs.uga.edu/pdfs/cuff_laura_e_201308_phd.pdf).
42. Cuff LE, Elliott KT, Seaton SC, Ishaq MK, Laniohan NS, Karls AC, et al. Analysis of IS1236-Mediated Gene Amplification Events in *Acinetobacter baylyi* ADP1. *Journal of Bacteriology*. 2012 Aug 15; 194(16):4395–405. <https://doi.org/10.1128/JB.00783-12> PMID: 22707704

43. Murphy KC, Campellone KG, Poteete AR. PCR-mediated gene replacement in *Escherichia coli*. *Gene*. 2000 Apr; 246(1–2):321–30. [https://doi.org/10.1016/s0378-1119\(00\)00071-8](https://doi.org/10.1016/s0378-1119(00)00071-8) PMID: 10767554
44. Eva Kickstein, Klaus Harms, Wilfried Wackernagel. Deletions of *recBCD* or *recD* influence genetic transformation differently and are lethal together with a *recJ* deletion in *Acinetobacter baylyi*. *Microbiology*. 2007; 153(7):2259–70.
45. Hulter N, Wackernagel W. Frequent integration of short homologous DNA tracks during *Acinetobacter baylyi* transformation and influence of transcription and *RecJ* and *SbcCD* DNases. *Microbiology*. 2008 Dec 1; 154(12):3676–85. <https://doi.org/10.1099/mic.0.2008/021378-0> PMID: 19047735
46. Overballe-Petersen S, Harms K, Orlando LAA, Mayar JVM, Rasmussen S, Dahl TW, et al. Bacterial natural transformation by highly fragmented and damaged DNA. *Proceedings of the National Academy of Sciences*. 2013 Dec 3; 110(49):19860–5. <https://doi.org/10.1073/pnas.1315278110> PMID: 24248361
47. Whitlock M, Schluter D. *The analysis of biological data*. Greenwood Village: Roberts and Co. Publishers; 2009.
48. Johnson ML. Nonlinear Least-Squares Fitting Methods. In: *Methods in Cell Biology* [Internet]. Academic Press; 2008. p. 781–805. (Biophysical Tools for Biologists, Volume One: In Vitro Techniques; vol.84).
49. Beck E, Ludwig G, Auerswald EA, Reiss B, Schaller H. Nucleotide sequence and exact localization of the neomycin phosphotransferase gene from transposon Tn5. *Gene*. 1982 Oct 1; 19(3):327–36. [https://doi.org/10.1016/0378-1119\(82\)90023-3](https://doi.org/10.1016/0378-1119(82)90023-3) PMID: 6295884
50. Lenski RE, Rose MR, Simpson SC, Tadler SC. Long-Term Experimental Evolution in *Escherichia coli*. I. Adaptation and Divergence During 2,000 Generations. *The American Naturalist*. 1991; 138(6):1315–41.
51. Starikova I, Al-Haroni M, Werner G, Roberts AP, Sorum V, Nielsen KM, et al. Fitness costs of various mobile genetic elements in *Enterococcus faecium* and *Enterococcus faecalis*. *Journal of Antimicrobial Chemotherapy*. 2013 Dec 1; 68(12):2755–65. <https://doi.org/10.1093/jac/dkt270> PMID: 23833178